

Homeobox Protein PROX1 Expression is Negatively Regulated by Histone Deacetylase 1 and c-JUN Complex in MDA-MB-231 Human Breast Cancer Cells

(AP-1 / c-JUN / HDAC1 / MDA-MB-231 / PROX1)

MUNKI JEONG, EUITAEK JUNG, SUKJIN OH, SOON YOUNG SHIN

Department of Biological Sciences, Sanghuh College of Life Sciences, Konkuk University, Seoul 05029, Republic of Korea

Abstract. Prospero homeobox 1 (PROX1) is a member of the homeobox transcription factor family that plays a critical role in the development of multiple tissues and specification of cell fate. PROX1 expression is differentially regulated based on the cellular context and plays an antagonistic role as a tumour promoter or suppressor in different tumour types. In human breast cancer, PROX1 expression is suppressed; however, the molecular mechanism by which it is down-regulated remains poorly understood. Here, we show that ectopic expression of PROX1 reduces the motility and invasiveness of MDA-MB-231 human breast cancer cells, suggesting that PROX1 functions as a negative regulator of tumour invasion in MDA-MB-231 cells. Treatment with histone deacetylase (HDAC) inhibitors up-regulates PROX1 mRNA

and protein expression levels. Knockdown of *HDAC1* using short hairpin RNA also up-regulates PROX1 mRNA and protein expression levels. We found that HDAC1 interacted with c-JUN at the activator protein (AP)-1-binding site located at –734 to –710 in the *PROX1* promoter region to suppress *PROX1* expression. In addition, c-JUN N-terminal kinase-mediated c-JUN phosphorylation was found to be crucial for silencing *PROX1* expression. In conclusion, PROX1 expression can be silenced by the epigenetic mechanism involved in the complex formation of HDAC1 and c-JUN at the AP-1 site in the *PROX1* promoter region in MDA-MB-231 human breast cancer cells. Therefore, this study revealed the epigenetic regulatory mechanism involved in the suppression of PROX1 expression in breast cancer cells.

Received July 1, 2022. Accepted October 9, 2023.

This study was supported by a National Research Foundation of Korea (NRF) grant funded by the Ministry of Science and ICT (2023R1A2C1003601) and by the KU Research Professor Program of the Konkuk University.

Corresponding author: Soon Young Shin, Department of Biological Sciences, Sanghuh College of Life Sciences, Konkuk University, 120 Neungdong-ro, Gwangjin-gu, Seoul 05029, Republic of Korea. Phone: (+82) 2 2030 7946; e-mail: shinsy@konkuk.ac.kr

Abbreviations: 3D – three-dimensional, ANOVA – analysis of variance, AP-1 – activator protein 1, EMSA – electrophoretic mobility shift assay, EMT – epithelial-to-mesenchymal transition, F-actin – filamentous actin, G-actin – globular actin, GAPDH – glyceraldehyde 3-phosphate dehydrogenase, GFP – green fluorescence protein, HAT – histone acetylase, HDAC – histone deacetylase, JNK – c-JUN N-terminal kinase, MAPK – mitogen-activated protein kinase, MMP – matrix metalloproteinase, NaBT – sodium butyrate, PROX1 – prospero homeobox 1, RT-PCR – reverse transcription-polymerase chain reaction, shRNA – short hairpin RNA, TIMP – tissue inhibitor of metalloproteinase, TNBC – triple-negative (oestrogen receptor-negative, progesterone receptor-negative, and EGF receptor-negative) breast cancer, VPA – valproic acid.

Introduction

Drosophila prospero is a homeobox domain-containing protein that plays a crucial role in determining the cell fate in the central nervous system (Doe et al., 1991). Prospero homeobox 1 (PROX1) is a mammalian homologue of Prospero that has a role in the development of the central nervous system, lens, heart, liver, pancreas, and lymphatic vasculature (Wigle et al., 1999; Sosa-Pineda et al., 2000; Burke and Oliver, 2002; Petrova et al., 2002; Lavado and Oliver, 2007; Risebro et al., 2009).

Alterations in PROX1 expression are involved in cancer development (Elsir et al., 2012). PROX1 expression levels are elevated in neuroblastoma, glioma, small cell lung carcinoma, gastrointestinal tract carcinoma, and liver carcinomas (Elsir et al., 2012). In contrast, PROX1 levels are decreased in sporadic primary breast cancer compared to normal breast tissues (Versmold et al., 2007). These studies suggest that PROX1 expression is differentially regulated depending on the cellular context and plays an antagonistic role as a tumour promoter or suppressor in different tumour types (Elsir et al., 2012).

The *PROX1* locus is located in the chromosomal region 1q32.2–q32.3 (Zinovieva et al., 1996), where frequent allelic imbalance has been reported in primary breast cancer (Benítez et al., 1997). DNA methylation is commonly associated with gene silencing via direct addition of a methyl group to cytosine in the DNA sequence (Bird, 2002). The *PROX1* locus is frequently hypermethylated on CpG islands, which are unmethylated GC-rich regions that possess high relative densities of CpG, of the first intron in neoplastic breast tissues (Versmold et al., 2007), suggesting that epigenetic modifications are involved in the *PROX1* expression in breast cancer.

Acetylation and deacetylation of lysine residues in the N-terminal tails of core histones are critical epigenetic modifications that affect the conformation of chromatin structure (Gujral et al., 2020). Histone acetyltransferases (HATs) and histone deacetylases (HDACs) add or remove acetyl groups from lysine residues in histones, respectively, thereby regulating the gene transcription. Histone deacetylation and DNA methylation of CpG islands are crucial epigenetic modifications that mediate transcriptional repression and gene silencing. Some studies suggest that histone modification is a prerequisite for the methylation of CpG islands (Fuks, 2005).

HDAC inhibitors exhibit therapeutic benefits in multiple cancers (West and Johnstone, 2014), including breast cancer (Munster et al., 2001; Marks, 2007). MDA-MB-231 is a triple-negative (oestrogen receptor-negative, progesterone receptor-negative, and EGF receptor-negative) breast cancer (TNBC) cell line that is highly invasive and aggressive among all breast cancer cell lines (Foulkes et al., 2010; Liu et al., 2015). In this study, we used the MDA-MB-231 cell line as a model cell line to study the epigenetic mechanism underlying the suppression of *PROX1* expression. We identified HDAC1 binding to c-JUN at the activator protein (AP)-1-binding site at –734 to –710 in the *PROX1* promoter.

Material and Methods

Cells and cell culture

TNBC MDA-MB-231 cells were obtained from the American Type Culture Collection (Manassas, VA). The cells were cultured in Dulbecco's modified Eagle's medium (DMEM) supplemented with 10 % foetal bovine serum (Hyclone, Logan, UT).

Reagents

The selective c-JUN N-terminal kinase (JNK) inhibitor, SP600125, was purchased from Tocris Bioscience (Ellisville, MO). The HDAC inhibitor, vorinostat, known as suberoylanilide hydroxamic acid (SAHA), AP-1 inhibitor, tanshinone II A (Tan II), HDAC class I inhibitor, sodium butyrate (NaBT), and HDAC class I and II inhibitor, valproic acid (VPA), were obtained from Sigma-Aldrich (St. Louis, MO). The luciferase assay kit was purchased from Promega (Madison, WI). Streptavidin-

agarose was obtained from Invitrogen (Carlsbad, CA). All other chemical reagents were purchased from Sigma-Aldrich.

Antibodies

Anti-*PROX1* antibody was purchased from R&D Systems (Minneapolis, MN). Anti-c-JUN, anti-HDAC1, and anti-V5 antibodies were obtained from Cell Signaling Technology (Danvers, MA). Anti-GAPDH antibody was purchased from Santa Cruz Biotechnology (Santa Cruz, CA).

Generation of MDA-MB-231 cells over-expressing PROX1

MDA-MB-231 cells were transfected with pBabe-puro/*PROX1*, encoding *PROX1*, using Lipofectamine 2000 (Invitrogen, Carlsbad, CA). Transfected cells were selected using 3 µg/ml puromycin for 3–4 weeks, and puromycin-resistant clones were isolated. *PROX1* over-expression was confirmed via immunoblotting. The resulting cells over-expressing *PROX1* were named MB231/*Prox1*. Cells transfected with an empty vector (pBabe-puro) were also generated as a control and named MB231/*Vec*.

Immunoblotting analysis

The cells were lysed in a buffer consisting of 20 mM HEPES (pH 7.2), 1 % Triton X-100, 10 % glycerol, 150 mM NaCl, 10 µg/ml leupeptin and 1 mM phenylmethylsulphonyl fluoride. Protein extracts (20 µg each) were separated using 8 % sodium dodecyl sulphate-polyacrylamide gel electrophoresis and transferred to nitrocellulose membranes. The blots were blocked with 5 % (w/v) non-fat dry milk in 0.05 % Tween 20 Tris-buffered saline (TTBS) for 30 min at 25 °C and incubated with primary antibodies overnight at 4 °C. After washing thrice with 0.1 % TTBS, the membranes were incubated with horseradish peroxidase-conjugated anti-mouse or anti-rabbit antibodies for 1 h at room temperature. The membranes were washed five times with 0.1 % TTBS and the bound antibodies were detected via chemiluminescence using an enhanced chemiluminescence detection system (Amersham Pharmacia Biotech, Piscataway, NJ).

Cell proliferation assay

Exponentially growing MB231/*Vec* and MB231/*Prox1* cells were seeded in a 96-well culture plate (1×10^3 cells/well). The proliferation rate was determined using a Cell Counting Kit-8 (CCK-8; Dojindo Molecular Technologies, Rockville, MD) based on the water-soluble tetrazolium salt WST-8 (2-[2-methoxy-4-nitrophenyl]-3-[4-nitrophenyl]-5-[2,4-disulfophenyl]-2H-tetrazolium, monosodium salt) as a substrate. At days 0, 1, 2, 3, and 4 after seeding, the CCK-8 solution was added, and the absorbance was measured at 450 nm using an Emax End-point ELISA Microplate Reader (Molecular Devices, San Jose, CA), according to the manufacturer's instructions.

Cell scratch assay

Cell migration was determined using a cell scratch assay, as previously described (Sethi et al., 2008). Briefly, MB231/Vec and MB231/Prox1 cells were cultured in a six-well plate and allowed to reach confluence. A scratch was made on the confluent cell layer with a pipette tip, followed by washing with serum-free DMEM to remove the cell debris. Cells were cultured in DMEM supplemented with 0.5 % foetal bovine serum, followed by gap closure for up to 36 h. Gap closure images were taken every 12 h using an EVOS FL Auto Cell Imaging System (Life Technologies, Carlsbad, CA). The closed-gap area was quantified using the ImageJ version 1.52a software (<http://imagej.nih.gov/ij/>; Center for Information Technology, National Institute of Health, Bethesda, MA).

Actin reorganization analysis

MB231/Vec and MB231/Prox1 cells were placed on glass coverslips and fixed with 4 % paraformaldehyde. After permeabilization with 0.3 % Triton X-100, polymerized microfilaments (filamentous actin, F-actin) were stained with rhodamine-conjugated phalloidin using a Visualization Biochem Kit (Cytoskeleton, Inc., Denver, CO), according to the manufacturer's instructions. Fluorescence images were captured using an EVOS FL fluorescence microscope (Advanced Microscopy Group; Bothell, WA).

Invasion assay using a three-dimensional (3D) spheroid culture model

Invasion assay was performed using a Cultrex 3D Spheroid Cell Invasion Assay kit (Trevigen, Inc., Gaithersburg, MD), as previously described (Shin et al., 2016). Briefly, after forming spheroids of MB231/Vec and MB231/Prox1 cells, they were embedded in Matrigel-based extracellular matrix components for seven

days. Invasive protrusions of spheroids into the surrounding extracellular matrix were visualized using an EVOS FL fluorescence microscope (Advanced Microscopy Group).

Reverse transcription-polymerase chain reaction (RT-PCR)

Cells were harvested and total RNA was isolated using NucleoZOL (Invitrogen). cDNA was synthesized from 1 µg of total RNA via RT using an iScript cDNA synthesis kit (Bio-Rad, Hercules, CA), according to the manufacturer's instructions. The gene-specific PCR primers are listed in Table 1. The PCR conditions used were as follows: hold for 4 min at 95 °C, followed by 30 s at 95 °C, 30 s at 60 °C, and 30 s at 72 °C for 30 cycles. The amplified products were separated using electrophoresis in 2 % agarose gel and visualized using ethidium bromide.

Generation of the human *PROX1* promoter-reporter

The 5'-regulatory region of human *PROX1* (ENST00000498508.6) spanning nucleotides (nt) -1077 to +33 was synthesized from human genomic DNA (Promega) using PCR with the following primers: 5'-AGATCTTTAAGAGCCACATTATCT-3' (forward) and 5'-CTCCGCTCCACAACAAGATT-3' (reverse). Hot-start PCR conditions used were as follows: hold for 10 min at 95 °C, followed by 30 s at 95 °C, 30 s at 60 °C, and 1 min at 72 °C for 35 cycles, according to the manufacturer's instructions (Enzynomics, Daejeon, Republic of Korea). PCR products were subcloned into a T&A vector (RBC Bioscience, New Taipei City, Taiwan), digested with restriction enzyme *Bgl*II (Enzynomics) and ligated into the pGL4.17 luciferase reporter vector (Promega), yielding pProx1-Luc(-1077/+33). The sequences of the promoter-reporter constructs were veri-

Table 1. Primer sequences for RT-PCR

Gene symbol	Forward primer	Reverse primer
<i>GAPDH</i>	ACCCACTCCTCCACCTTTG	CTCTTGTGCTCTTGCTGGG
<i>PROX1</i>	CAGATGGAGAAGTACGCAC	CAAGAGCTGCTTCATGAGTAG
<i>HDAC1</i>	CCAAGTACCACAGCGATGAC	GCCAAGACGATATCATTGACG
<i>aSMA</i>	GATCACCATCGGGAATGAACGC	CTTAGAAGCATTTCGGGTGGAC
<i>VIM</i>	TGGCACGTCTTGACCTTGAA	GGTCATCGTGATGCTGAGAA
<i>SNAIL1</i>	CTGCAGGACTCTAATCCAG	CGAGAGACTCCGGTTCCTA
<i>MMP1</i>	CAAAATCCTGTCCAGCCCATCG	TTCGTAAGCAGCTTCAAGCCC
<i>MMP2</i>	CAATACCTGAACACCTT	CTGTATGTGATCTGGTT
<i>MMP9</i>	AGATTCCAAACCTTTGAG	CGCCTTGGAAGATGAATG
<i>TIMP1</i>	TTCGTGGGGACACCAGAAGTCAAC	TGGACACTGTGCAGGCTTCAGTTC
<i>TIMP3</i>	GCCTTCTGCAACTCCGAC	GCCCATCCTCGGTACCAG
<i>TIMP4</i>	CCCTGCTGACACTGAAAA	CTGTAGCAAGTCGGGATC

fied by DNA sequencing at MacroGen (Seoul, Republic of Korea). The AP-1-binding motif was analysed using the TOMTOM software (<http://meme.nbcr.net/meme/cgi-bin/tomtom.cgi>).

Luciferase promoter-reporter assay

MDA-MB-231 cells were transfected with 0.1 µg pProx1-Luc(-1077/+33) plasmid using Lipofectamine 2000 (Invitrogen). After 48 h of transfection, the cells were either left untreated or treated with HDAC inhibitors for 8 h, and luciferase activity was measured using a luminometer (Centro LB960; Berthold Tech, Bad Wildbad, Germany). The relative luciferase activity of the untreated sample was designated as 1.

Silencing of HDAC1 and c-JUN using RNA interference

MDA-MB-231 cells were incubated with a lentiviral short hairpin RNA (shRNA) targeting HDAC1 (GCTGCTCAACTATGGTCTCTAC; MISSION shRNA TRCN0000004818; Sigma-Aldrich, St. Louis, MO) or c-JUN (TAGTACTCCTTAAGAACACAA; MISSION shRNA TRCN0000010366; Sigma-Aldrich), according to the manufacturer's instructions. After two weeks, the cells were collected, and silencing of HDAC1 or c-JUN expression was verified via immunoblotting.

Electrophoretic mobility shift assay (EMSA)

EMSA was performed using a LightShift chemiluminescence EMSA kit (Thermo Fisher Scientific, Waltham, MA). A biotin-labelled deoxyoligonucleotide probe corresponding to the AP-1-binding sequence (5'-AGATAA ACTGGGACTCAGCCAATGT-biotin-3') at position -734 to -710 of the *PROX1* promoter region was synthesized by MacroGen. MDA-MB-231 cells were transfected with 5 µg of the expression plasmid for c-JUN (pcDNA3.1/V5-His-c-JUN) or green fluorescent protein (pMAX/GFP) as a control. Nuclear extracts (3 µg samples) were prepared and mixed with 50 fmol biotin-labelled oligonucleotide probes and 1 µg poly(dI-dC) (Amersham Biosciences, Piscataway, NJ). For the competition assay, 2.5 and 5 pmol of the unlabelled AP-1-binding probe (competitor) were added. DNA-protein complexes were separated in non-denaturing 6 % polyacrylamide gel, and biotin-labelled DNA was detected using streptavidin-conjugated horseradish peroxidase and chemiluminescence reagents, according to the manufacturer's instructions (Thermo Fisher Scientific, Waltham, MA).

Immunoprecipitation assay

For immunoprecipitation assay, MDA-MB-231 cells were transfected with an expression plasmid encoding c-JUN (pcDNA3.1/V5-His-c-JUN) or GFP as a control (pMAX/GFP). After 48 h, the cells were collected, and total proteins were lysed in a lysis buffer (50 mM Tris-HCl, pH 7.9, 10 mM KCl, 400 mM NaCl, 1 mM EDTA, 0.2 % NP-40, 10 % glycerol, 1 mM phenylmethylsul-

phonyl fluoride and a cocktail of protease inhibitors). The cell lysates were incubated with the anti-V5 antibody (Cell Signaling Technology) overnight at 4 °C. Antibody-bound protein complexes were precipitated using Pierce Protein A Plus agarose (Thermo Fisher Scientific). Agarose beads were washed thrice with the lysis buffer and heated in a sodium dodecyl sulphate (SDS) sample loading buffer at 95 °C for 5 min. The eluted samples were separated by SDS-polyacrylamide gel electrophoresis, and immunoblotting analysis was performed using anti-V5 and anti-HDAC1 antibodies. Blots were visualized using an enhanced chemiluminescence detection system (Amersham Pharmacia Biotech).

Statistical analysis

Statistical significance was analysed using GraphPad Prism version 9.3.1 (GraphPad Software Inc., La Jolla, CA). Statistical significance was set at $P < 0.05$.

Results

Over-expression of PROX1 suppresses the invasiveness of MDA-MB-231 cells

Silencing PROX1 expression increases the vascularization in thyroid cancer cells (Rudzińska and Czarnocka, 2020) and enhances matrix metalloproteinase (MMP)-14 expression, which is involved in angiogenesis and tumour invasion in breast cancer cells (Gramolelli et al., 2018), suggesting that PROX1 plays a tumour-suppressive role in breast cancer. To confirm the role of PROX1 as a tumour suppressor in breast cancer, we used MDA-MB-231 breast cancer cells over-expressing PROX1 (Fig. 1A). We observed that the proliferation rate of MDA-MB-231 cells over-expressing PROX1 (MB231/Prox1) was similar to that of the parental and empty vector-transfected cells (MB231/Vec) (Fig. 1B). Notably, MB231/Prox1 cells showed reduced gap closure compared to that in MB231/Vec cells (Fig. 1C), suggesting that PROX1 inhibited the motility of MDA-MB-231 cells.

Cell motility is a critical characteristic of cancer cell invasion and metastasis. Cell migration largely depends on actin cytoskeleton dynamics in response to changes in cell contractility. Monomeric globular actin (G-actin) polymerizes to F-actin during the cell movement to build higher-order structures, such as stress fibres, lamellipodia, and filopodia (Merino et al., 2020). To determine whether PROX1 affects actin cytoskeletal rearrangement, we visualized F-actin fibres using rhodamine-conjugated phalloidin, an F-actin binding heptapeptide, in MDA-MB-231 cells over-expressing PROX1. Polarized F-actin-rich protrusions (arrows) were reduced in PROX1-over-expressing cells compared to those in vector-transfected control cells (Fig. 1D). Enhanced cell motility is closely related to the invasion and metastasis of cancer cells. To investigate the role of PROX1 in tumour invasion, we used a Matrigel-based 3D spheroid culture system that closely resembled the environment

inside the tumour mass *in vivo*. MDA-MB-231 cells formed aggregates at day 1 in the 3D Matrigel and appeared to be non-invasive (Fig. 1E, top panels). After seven days of culture, control cells came out of the spheroid and invaded into the surrounding matrix, but *PROX1*-expressing cells almost lost their invasive capability (Fig. 1E, bottom panels).

Epithelial-to-mesenchymal transition (EMT) has been implicated in promoting the migration and inva-

sion of epithelial tumour cells (Zhang and Weinberg, 2018). Alpha-smooth muscle actin, vimentin, and snail are typical EMT markers (Pinkas and Leder, 2002; Kudo-Saito et al., 2009; Suarez-Carmona et al., 2017). MMPs are a family of proteinases involved in the degradation of the extracellular matrix (Cockett et al., 1998) and in the promotion of tumour growth, invasion, and metastasis (Chambers, 1997; Westermarck, 1999). Tissue inhibitors of metalloproteinases (TIMPs) include

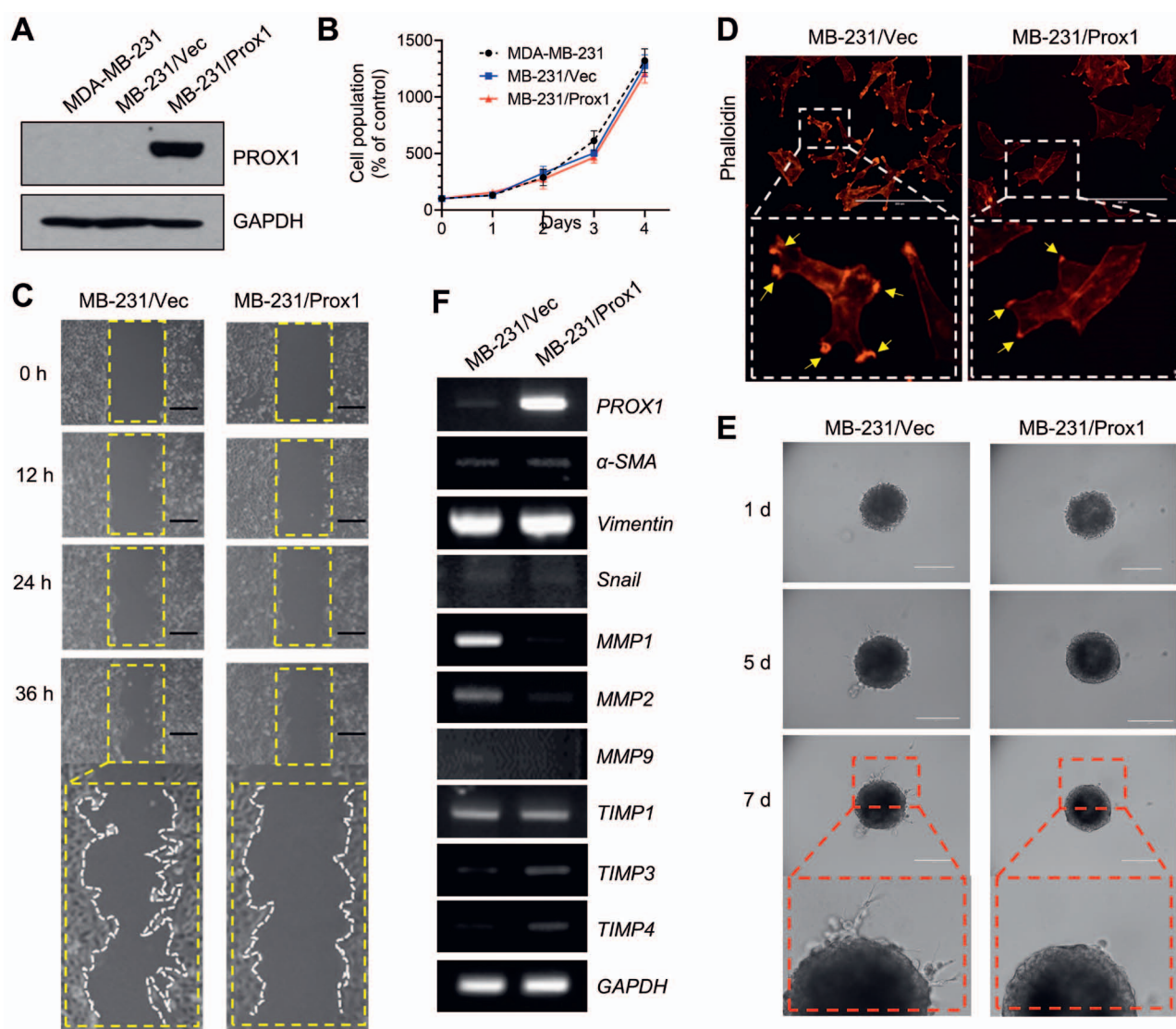


Fig. 1. Effect of ectopic expression of prospero homeobox 1 (*PROX1*) on the inhibition of invasiveness of MDA-MB-231 cells. **(A)** Immunoblotting analysis. MDA-MB-231 cells were transfected with empty vector pBabe-puro (MB231/Vec) or pBabe-puro/*PROX1* encoding *PROX1* (MB231/*Prox1*). *PROX1* protein levels were determined via immunoblotting. Glyceraldehyde 3-phosphate dehydrogenase (GAPDH) was used as an internal control. **(B)** Cell proliferation assay. MB231/Vec and MB231/*Prox1* cells were seeded into a 96-well plate, and the relative cell proliferation rate was determined using a Cell Count Kit-8. The data represent the mean \pm standard deviation (SD) (N = 3). **(C)** Motility of MB231/Vec and MB231/*Prox1* cells was analysed using a cell scratch assay. Dotted lines indicate the scraped boundaries at the beginning of the experiment. **(D)** MB231/Vec and MB231/*Prox1* cells were stained with rhodamine-phalloidin (1 : 100) and their actin rearrangement was analysed. Arrows indicate polarized filamentous actin (F-actin). Scale bar, 200 μ m. **(E)** MB231/Vec and MB231/*Prox1* cells were cultured in three-dimensional spheroids in Matrigel-based extracellular matrix contents. Protrusions of invasive cells were captured using an EVOS FL Auto Cell Imaging System.

endogenous MMP inhibitors (Kähäri and Saarialho-Kere, 1999). RT-PCR analysis showed that over-expression of PROX1 did not alter the expression levels of EMT markers, but down-regulated MMP-1 and MMP-2 levels while up-regulating TIMP-3 and TIMP-4 levels (Fig. 1F). These data suggest that PROX1 may function as a tumour suppressor in MDA-MB-231 cells via a mechanism involving negative regulation of the invasive capability of tumour cells.

HDAC inhibitors increase PROX1 expression

The mechanism by which PROX1 expression is silenced in cancer cells remains unclear. DNA hypermethylation of CpG islands is commonly associated with gene silencing (Bird, 2002). The promoter region of *PROX1* contains CpG islands within 1 kb of the transcription start site (Vermold et al., 2007). HDAC interacts with methylated DNA and deacetylates the histone tail, thereby linking DNA methylation to epigenetic gene silencing (Nan et al., 1998). In humans, there are 18 HDACs divided into four classes: class I (HDAC1–3, and 8), class II (HDAC4–7, 9, and 10), class III (Sirtuin 1–7), and class IV (HDAC11) (Seto and Yoshida, 2014). Therefore, we speculated that HDACs may play a role

in modulating *PROX1* transcription. To test this possibility, we isolated the 5'-regulatory region of human *PROX1*, located 1077 bp upstream of the transcriptional start site, and subcloned it into the pGL4.17-Luc reporter vector, yielding pProx1-Luc(-1077/+33). We transfected this construct into MDA-MB-231 cells and examined the effects of various HDAC inhibitors, including SAHA (Class I, II, and IV inhibitors), VPA (Class I and II HDAC inhibitors), and NaBT (Class I HDAC inhibitor), on *PROX1* promoter-reporter activity. We found that all tested HDAC inhibitors significantly (all $P < 0.001$) increased the *PROX1* promoter-reporter activity (Fig. 2A). Furthermore, RT-PCR and immunoblotting analyses confirmed the ability of HDAC inhibitors to enhance *PROX1* mRNA (Fig. 2B) and protein (Fig. 2C) expression levels, suggesting that HDACs are involved in regulating *PROX1* gene transcription.

To further determine the role of HDACs in inhibiting *PROX1* expression, we silenced HDAC1 expression using a shRNA in MDA-MB-231 cells. We found that *PROX1* mRNA (Fig. 2D) and protein (Fig. 2E) expression levels were enhanced in cells transfected with HDAC1-specific shRNA (shHDAC1) compared to those transfected with scrambled shRNA (shCT), suggesting

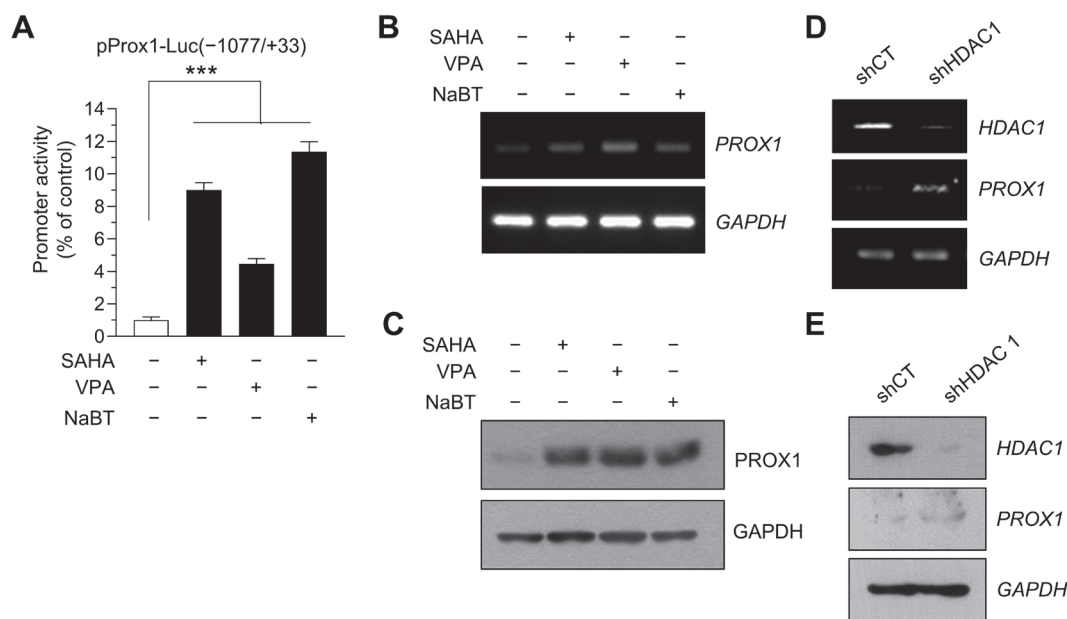


Fig. 2. Effect of histone deacetylase (HDAC) inhibitors on the increase in PROX1 expression. (A) *PROX1* promoter-reporter assay. MDA-MB-21 cells were transiently transfected with 0.1 μ g human *PROX1* promoter-reporter plasmid, pProx1-Luc(-1077/+33). After 48 h, the cells were treated with 5 μ M suberoylanilide hydroxamic acid (SAHA), 4 mM valproic acid (VPA), and 4 mM sodium butyrate (NaBT). After 48 h, the cells were harvested and luciferase reporter activities were measured. The data represent the mean \pm SD. *** $P < 0.001$, ** $P < 0.01$. (B–C) MDA-MB-21 cells were treated with 5 μ M SAHA, 4 mM VPA, and 4 mM NaBT. After 12 h (B) and 24 h (C), the cells were harvested, and PROX1 mRNA and protein levels were determined using reverse transcription-polymerase chain reaction (RT-PCR) (B) and immunoblotting analysis (C), respectively. GAPDH was used as an internal control. (D–E) MDA-MB-21 cells expressing the control scramble short hairpin RNA (shRNA) (shCT) or shRNA targeting HDAC1 (shHDAC1) were harvested, and HDAC1 and PROX1 mRNA and protein levels were determined using RT-PCR (D) and immunoblotting analysis (E), respectively. GAPDH was used as an internal control.

the negative role of HDACs in *PROX1* expression. These data indicate that aberrant HDAC activity contributes to the silencing of *PROX1* expression.

HDAC1 interacts with c-JUN at the AP-1-binding site in the PROX1 promoter

HDAC1 has been shown to interact with c-JUN (Sanna and Galeotti, 2018). c-JUN is an AP-1 subunit that binds to the AP-1 site along with other AP-1 family members. We identified a putative AP-1-binding site at position -734 to -710 in the 5'-regulatory region of *PROX1* (Fig. 3A). To determine whether c-JUN binds to the AP-1 site at -734 to -710, we performed an EMSA using nuclear extracts of MDA-MB-231 cells transfected with the c-JUN expression plasmid. Transient expression of c-JUN complexed with a biotinylated AP-1-binding probe corresponding to the AP-1 motif sequence at -734 to -710 and competed for the unlabelled probe (Fig. 3B), suggesting that the AP-1 motif at -734 to -710 is a functional *cis*-acting element that binds to c-JUN.

To determine the role of c-JUN in *PROX1* expression, we transiently co-transfected the pProx1-Luc (-1077/+33) reporter and an expression plasmid encoding c-JUN (pcDNA3.1 V5-His/c-JUN) or GFP as a control (pMAX/GFP) into MDA-MB-231 cells. The promoter-reporter assay showed that the transient expression of c-JUN significantly reduced ($P < 0.001$) the *PROX1* promoter-reporter activity compared to that of GFP (Fig. 3C). In contrast, knockdown of c-JUN expression using shRNA (shJun) increased the *PROX1* mRNA (Fig. 3D) and protein (Fig. 3E) levels compared to the control shRNA (shCT) expression levels.

We then tested whether c-JUN was associated with HDAC1 using HEK293 cells, as they exhibit higher transfection efficiency than MDA-MB-231 cells. We performed an immunoprecipitation assay using nuclear extracts of HEK293 cells transfected with GFP expression plasmid or V5-tagged c-JUN (V5-JUN). After whole cell lysates were immunoprecipitated with an anti-JUN antibody, the immunoprecipitates were analysed via immunoblotting with an anti-V5 or anti-HDAC1 antibody. We found that endogenous HDAC1 co-immunoprecipitated with c-JUN (Fig. 3F). These results suggest that c-JUN interacts with HDAC1 at the AP-1 site located at position -734 to -710 to repress *PROX1* expression in MDA-MB-231 cells.

Inhibition of JNK increases PROX1 mRNA and protein levels

JNK phosphorylates c-JUN and forms homo- or heterodimers with other AP-1 family members to form an active AP-1 complex. To investigate whether JNK is involved in the suppression of *PROX1* expression via c-JUN phosphorylation, we tested the effect of the JNK inhibitor, SP600125, on *PROX1* expression. Following SP600125 treatment, *PROX1* mRNA levels peaked within 6 h and decreased slowly, but remained elevated

for 24 h (Fig. 4A), whereas the protein levels of PROX1 were readily detected after 24 h of stimulation (Fig. 4B). However, other mitogen-activated protein kinase inhibitors, such as the MEK inhibitor, U0126, and p38 kinase inhibitor, SB600125, had little effect on *PROX1* mRNA expression (Fig. 4C). These data suggest that JNK-mediated c-JUN phosphorylation is involved in the silencing of *PROX1* expression.

Discussion

The present study demonstrated that PROX1 expression can be silenced by the epigenetic mechanism involved in HDAC1 and c-JUN complex formation at the AP-1 site in the *PROX1* promoter region in MDA-MB-231 human breast cancer cells. These findings may aid in understanding the molecular mechanism underlying the aberrant silencing of *PROX1* expression in breast cancer. HDAC inhibitors may be used as promising chemotherapeutic agents to prevent the invasion and metastasis of breast cancer cells by restoring PROX1 expression. However, further investigations are necessary to determine the mechanism regulating the interaction between HDAC1 and c-JUN at the AP-1 site of the *PROX1* promoter and whether HDAC1 and c-JUN complexes are formed *in vivo*.

In breast cancer, PROX1 functions as a tumour suppressor and is frequently silenced due to hypermethylation of CpG islands within the *PROX1* gene in neoplastic breast tissues (Versmold et al., 2007). This suggests that the loss of PROX1 function may contribute to the development and progression of breast cancer. In contrast, in hepatocellular carcinoma (HCC), PROX1 exhibits strong up-regulation in hepatic cancer cells. PROX1 up-regulation triggers an EMT response, promoting HCC invasion and metastasis (Liu et al., 2013), indicating that PROX1 plays a role in promoting cancer progression in the context of HCC. Therefore, PROX1 appears to have a complex role in cancer, acting as both a tumour suppressor and a promoter depending on the specific cancer types and cellular context. Further research is needed to better understand the precise mechanisms and factors that govern PROX1 functions in various types of cancer.

Conflicts of interest

The authors declare no conflicts of interest regarding the publication of this paper.

References

- Benítez, J., Osorio, A., Barroso, A. et al. (1997) A region of allelic imbalance in 1q31-32 in primary breast cancer coincides with a recombination hot spot. *Cancer Res.* **57**, 4217-4220.
- Bird, A. (2002) DNA methylation patterns and epigenetic memory. *Genes Dev.* **16**, 6-21.
- Burke, Z., Oliver, G. (2002) Prox1 is an early specific marker for the developing liver and pancreas in the mammalian foregut endoderm. *Mech. Dev.* **118**, 147-155.

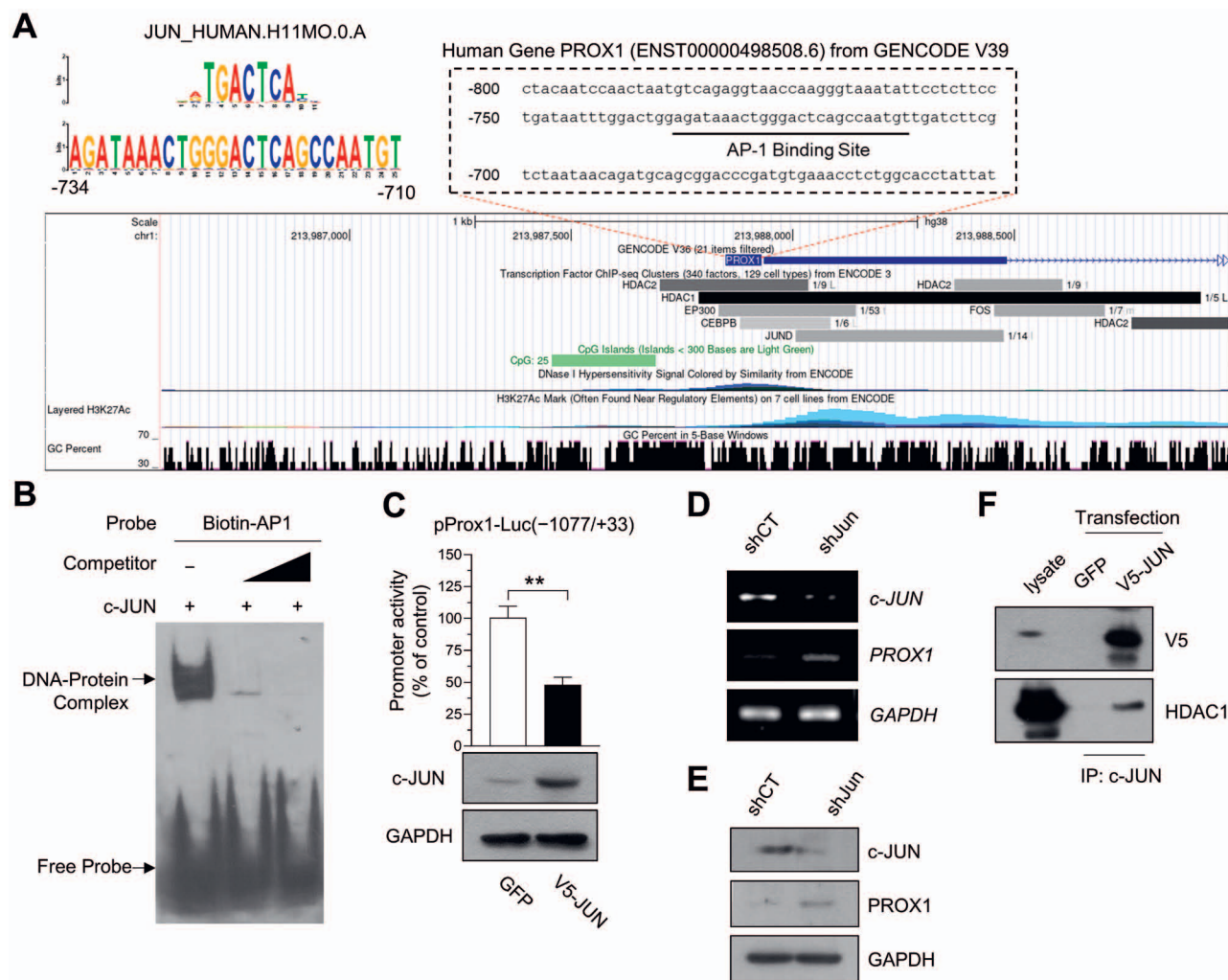


Fig. 3. HDAC1 interacts with c-JUN at the activator protein (AP)-1-binding site in the *PROX1* promoter. **(A)** Screenshot of UCSC Genome browser showing transcription factor ChIP-seq clusters including HDAC1 and HDAC2 (grey and black bars), CpG islands (green bar), DNase hypersensitivity signal (blue), acetylation of histone 3 at lysine-27 (H3K27Ac) mark (sky blue), and GC content (bottom bar graph) around the *PROX1* promoter region. The sequence of the 5'-regulatory region between the positions -800 and -651 nucleotides of the *PROX1* from GENCODE V39 is shown in the dotted box (top right). The AP-1-binding site at -734/-710 (underlined) was analysed using the TomTom software (top left). **(B)** Electrophoretic mobility shift assay (EMSA) analysis. MDA-MB-21 cells were transiently transfected with the c-JUN expression plasmid. After 48 h, the cells were harvested, and nuclear extracts (3 μ g) were incubated with 50 fmole biotin-labelled AP-1-binding oligonucleotide probes corresponding to position -734 to -710 of *PROX1*. For the competition assay, 2.5 or 5 pmole unlabelled oligonucleotides (Competitor) were added prior to addition of the labelled probes. After electrophoresis in non-denaturing 6% polyacrylamide gels and transfer to blotting membranes, protein-DNA complexes were visualized using streptavidin-conjugated horseradish peroxidase using a LightShift Chemiluminescence EMSA kit. **(C)** MDA-MB-231 cells were co-transfected with 5 μ g of pProx1-Luc (-1077/+33) and 5 μ g of pcDNA3.1/V5-His-c-JUN plasmids or pMAX/GFP (as a control). After 48 h, cells were collected, and luciferase activity was measured. The data represent the mean \pm SD. *** $P < 0.001$. Expression of c-JUN was confirmed via immunoblotting (bottom panels). GAPDH was used as an internal control. **(D-E)** MDA-MB-231 cells expressing the control shRNA (shCT) or c-JUN shRNA (shJun) were harvested, and c-JUN and *PROX1* mRNA and protein levels were determined using RT-PCR **(D)** and immunoblotting analysis **(E)**, respectively. GAPDH was used as an internal control. **(F)** HEK293 cells were transiently transfected with the expression plasmids for c-JUN (pcDNA3.1/V5-His-c-JUN) or green fluorescence protein (GFP) as a control (pMAX/GFP). After 48 h, cells were harvested and whole lysates were immunoprecipitated with a normal mouse IgG or anti-V5 antibody using protein A agarose beads. The immunoprecipitates were eluted using the sodium dodecyl sulphate (SDS) sample loading buffer and subjected to immunoblotting with anti-c-JUN and anti-HDAC1 antibodies. IP, immunoprecipitation.



Fig. 4. Effect of the inhibition of c-JUN N-terminal kinase (JNK) expression on the increase in *PROX1* expression. **(A)** MDA-MB-231 cells were treated with 5 μ M U0126, 20 μ M SB203580, or 25 μ M SP600125. After 12 h, cells were harvested and *PROX1* mRNA expression was determined using RT-PCR. *GAPDH* was used as an internal control. **(B, C)** MDA-MB-231 cells were treated with 25 μ M SP600125 for different time periods (0–24 h). After 12 h **(B)** and 24 h **(C)**, the cells were harvested, and *PROX1* mRNA and protein levels were determined using RT-PCR **(B)** and immunoblotting analysis **(C)**, respectively. *GAPDH* was used as an internal control.

- Chambers, A. F., Matrisian, L. (1997) Changing views of the role of matrix metalloproteinases in metastasis. *J. Natl. Cancer Inst.* **89**, 1260-1270.
- Cockett, M. I., Murphy, G., Birch, M. et al. (1998) Matrix metalloproteinases and metastatic cancer. *Biochem. Soc. Symp.* **63**, 295-313.
- Doe, C. Q., Chu-LaGraff, Q., Wright, D. M. et al. (1991) The prospero gene specifies cell fates in the *Drosophila* central nervous system. *Cell* **65**, 451-464.
- Elsir, T., Smits, A., Lindström, M. S. et al. (2012) Transcription factor *PROX1*: its role in development and cancer. *Cancer Metastasis Rev.* **31**, 793-805.
- Foulkes, W. D., Smith, I. E., Reis-Filho, J. S. (2010) Triple-negative breast cancer. *N. Engl. J. Med.* **363**, 1938-1948.
- Fuks, F. (2005) DNA methylation and histone modifications: teaming up to silence genes. *Curr. Opin. Genet. Dev.* **15**, 490-495.
- Gramolelli, S., Cheng, J., Martinez-Corral, I. et al. (2018) *PROX1* is a transcriptional regulator of *MMP14*. *Sci. Rep.* **8**, 1-13.
- Gujral, P., Mahajan, V., Lissaman, A. C. et al. (2020) Histone acetylation and the role of histone deacetylases in normal cyclic endometrium. *Reprod. Biol. Endocrinol.* **18**, 84.
- Kähäri, V. M., Saarialho-Kere, U. (1999) Trends in molecular medicine: matrix metalloproteinases and their inhibitors in tumour growth and invasion. *Ann. Med.* **31**, 34-45.
- Kudo-Saito, C., Shirako, H., Takeuchi, T. et al. (2009) Cancer metastasis is accelerated through immunosuppression during Snail-induced EMT of cancer cells. *Cancer Cell* **15**, 195-206.
- Lavado, A., Oliver, G. (2007) *Prox1* expression patterns in the developing and adult murine brain. *Dev. Dyn.* **236**, 518-524.
- Liu, Y., Zhu, P., Wang, Y. et al. (2015) Antimetastatic therapies of the polysulfide diallyl trisulfide against triple-negative breast cancer (TNBC) via suppressing *MMP2/9* by blocking NF- κ B and ERK/MAPK signaling pathways. *PLoS One* **10**, e0123781.
- Liu, Y., Zhang, J.-B., Qin, Y. et al. (2013) *PROX1* promotes hepatocellular carcinoma metastasis by way of up-regulating hypoxia-inducible factor 1 α expression and protein stability. *Hepatology* **58**, 692-705.
- Marks, P. A. (2007) Discovery and development of SAHA as an anticancer agent. *Oncogene* **26**, 1351-1356.
- Merino, F., Pospich, S., Raunser, S. (2020) Towards a structural understanding of the remodeling of the actin cytoskeleton. *Semin. Cell Dev. Biol.* **102**, 51-64.
- Munster, P. N., Troso-Sandoval, T., Rosen, N. et al. (2001) The histone deacetylase inhibitor suberoylanilide hydroxamic acid induces differentiation of human breast cancer cells. *Cancer Res.* **61**, 8492-8497.
- Nan, X., Ng, H. H., Johnson, C. A. et al. (1998) Transcriptional repression by the methyl-CpG-binding protein MeCP2 involves a histone deacetylase complex. *Nature* **393**, 386-389.
- Petrova, T. V., Mäkinen, T., Mäkelä, T. P. et al. (2002) Lymphatic endothelial reprogramming of vascular endothelial cells by the *Prox-1* homeobox transcription factor. *EMBO J.* **21**, 4593-4599.
- Pinkas, J., Leder, P. (2002) MEK1 signaling mediates transformation and metastasis of EpH4 mammary epithelial cells independent of an epithelial to mesenchymal transition. *Cancer Res.* **62**, 4781-4790.
- Risebro, C. A., Searles, R. G., Melville, A. A. et al. (2009) *Prox1* maintains muscle structure and growth in the developing heart. *Development* **136**, 495-505.
- Rudzińska, M., Czarnocka, B. (2020) The impact of transcription factor prospero homeobox 1 on the regulation of thyroid cancer malignancy. *Int. J. Mol. Sci.* **21**, 3220.
- Sanna, M. D., Galeotti, N. (2018) The HDAC1/c-JUN complex is essential in the promotion of nerve injury-induced neuropathic pain through JNK signaling. *Eur. J. Pharmacol.* **825**, 99-106.
- Sethi, G., Sung, B., Aggarwal, B. B. (2008) TNF: a master switch for inflammation to cancer. *Front. Biosci.* **13**, 5094-5107.
- Seto, E., Yoshida, M. (2014) Erasers of histone acetylation: the histone deacetylase enzymes. *Cold Spring Harb. Perspect. Biol.* **6**, a018713.

- Shin, S. Y., Kim, C. G., Jung, Y. J. et al. (2016) The UPR inducer DPP23 inhibits the metastatic potential of MDA-MB-231 human breast cancer cells by targeting the Akt-IKK-NF- κ B-MMP-9 axis. *Sci. Rep.* **6**, 34134.
- Sosa-Pineda, B., Wigle, J. T., Oliver, G. (2000) Hepatocyte migration during liver development requires Prox1. *Nat. Genet.* **25**, 254-255.
- Suarez-Carmona, M., Lesage, J., Cataldo, D. et al. (2017) EMT and inflammation: inseparable actors of cancer progression. *Mol. Oncol.* **11**, 805-823.
- Versmold, B., Felsberg, J., Mikeska, T. et al. (2007) Epigenetic silencing of the candidate tumor suppressor gene PROX1 in sporadic breast cancer. *Int. J. Cancer* **121**, 547-554.
- West, A. C., Johnstone, R. W. (2014) New and emerging HDAC inhibitors for cancer treatment. *J. Clin. Invest.* **124**, 30-39.
- Westermarck, J., Kähäri, V. M. (1999) Regulation of matrix metalloproteinase expression in tumour invasion. *FASEB J.* **13**, 781-792.
- Wigle, J. T., Chowdhury, K., Gruss, P. et al. (1999) Prox1 function is crucial for mouse lens-fibre elongation. *Nat. Genet.* **21**, 318-322.
- Zhang, Y., Weinberg, R. A. (2018) Epithelial-to-mesenchymal transition in cancer: complexity and opportunities. *Front. Med.* **12**, 361-373.
- Zinovieva, R. D., Duncan, M. K., Johnson, T. R. et al. (1996) Structure and chromosomal localization of the human homeobox gene Prox 1. *Genomics* **35**, 517-522.